Viscoacoustic reverse time migration in tilted TI media with attenuation compensation

Ali Fathalian, Daniel O. Trad and Kristopher A. Innanen

ABSTRACT

Simulation of wave propagation in an anisotropic viscoacoustic medium is an important problem, for instance within Q-compensated reverse-time migration. Processes of attenuation, dispersion, and anisotropic influence all aspects of seismic wave propagation, degrading resolution of migrated images. We present a new approach of the viscoacoustic wave equation in the time domain to explicitly separate amplitude attenuation with phase dispersion and develop a theory of viscoacoustic reverse time migration (Q-RTM) in tilted TI media. Because of this separation, we would be able to compensate the amplitude loss effect, the phase dispersion effect, or both effects. In the Q-RTM implementation, the attenuation-compensated operator was constructed by reversing the sign of amplitude attenuation. Using the TI approximation and ignoring all spatial derivatives of the anisotropic symmetry axis direction leads to instabilities in some area of the model with the rapid variations in the symmetry axis direction. A solution to this problem is proposed that involves using a selective anisotropic parameter equating in the model to reduce the difference of Thompson parameters in areas of rapid changes in the symmetry axes. The scheme is tested on a layer model and a modified acoustic Marmousi velocity model with a 2-4 staggered grid. We validate and examine the response of this approach by using it within a reverse time migration scheme adjusted to compensate for attenuation. The amplitude loss in the wavefield at the source and receivers due to attenuation can be recovered by applying compensation operators on the measured receiver wavefield. After correcting for the effects of anisotropy and viscosity, numerical test on synthetic data illustrates the higher resolution images with improved amplitude and the correct locations of reflectors, particularly beneath high-attenuation layers.

INTRODUCTION

Attenuation is an increasingly indispensable component of wavefield simulation in seismic exploration and monitoring applications. It is a key element in many recent instances of data modeling, reverse time migration (RTM). To consider the anisotropic media, the isotropic acoustic assumption for seismic processing and imaging method is not useful and affected the resolution and placed images of subsurface structures (Zhou et al., 2006). Therefore, it is necessary to focus on the anisotropy and viscosity for complex media to obtain a significant improvement in image resolution and positioning. There are to way to consider the anisotropic medium, the pseudo-acoustic wave equation and the pure acoustic wave equation. Alkhalifah (1998, 2000) derived the pseudo-acoustic wave equation from the dispersion relation by setting the shear-wave velocity along the anisotropy symmetry axis to be zero. Although the VTI wave equation is used to image structures which have similar properties with a VTI media (Crampin, 1984), but may not be satisfied in anisotropic dipping layers. The TTI equations have been derived from VTI equations by assuming the symmetry axis is non-vertical and locally variable (Fletcher et al., 2008; Zhang and Zhang, 2008). The TI wave equations with the zero value of S_V wave's velocity on

the axis symmetry can't remove the effect of the residual shear wave, so the instability occurs. Fletcher et al. (2009) proposed the equations by adding non-zero S-wave velocity terms to solve the problem. To stabilize wave propagation and reduce shear wave artifacts the parameters models of anisotropy can be smoothing before numerical simulation, and setting $\varepsilon = \delta$ in the regions around source and areas with the high symmetry axis gradient (Zhang and Zhang, 2008; Yoon et al., 2010). However, to investigate the RTM images in anisotropic viscoelastic medium, generally, the focus is on the anisotropy or viscosity. In this work, we focus on both anisotropy and viscosity to obtain the accurate RTM images.
To avoid the difficulty of stabilising the wave propagation, Fletcher et al. (2012) proposed the separate amplitude and phase filters to twice-extrapolated source and receiver wavefields to compensate for amplitude and phase effects. Dutta and Schuster (2014) adopted a least-squares RTM (LSRTM) approach for attenuation compensation based on an standard linear solid (SLS) model and its adjoint operator (Blanch and Symes, 1995) with a simplified stress-Strain relation. Zhu and Harris (2014) introduced a constant-Q viscoacoustic wave equation with separate fractional Laplacians, and applied it to the problem of Q-compensated RTM. Although RTM based on two-way wave equation is considered as a standard migration tool to image complex geologic regions, we try to formulate a time-domain viscoacoustic wave equation with attenuation correction in RTM(Q-RTM).
In this paper, we present a new approach of anisotropic viscoacoustic wave equation for attenuating media in the time domain based on SLS model. This equation describes the constant-Q wave propagation and contains independent terms for phase dispersion and amplitude attenuation. The attenuation effects compensate in the reconstructed wavefield by reversing the sign of amplitude loss operator and unchanged sign of dispersion operator. The new approach of viscoacoustic wave equation in TTI media develops a methodology of Q-RTM that can compensate amplitude attenuation and phase dispersion effects in the migrated images. We use two synthetic examples to test the accuracy of the proposed the method in application to imaging and demonstrate that Q-RTM compensates for amplitude attenuation and phase dispersion in the receiver wavefields when using the crosscorrelation imaging condition. This article is organized as follows. In the second section, we derive the viscoacoustic wave equation in TTI media. Next, we propose the formulation of Q-RTM and discuss the compensation of attenuation effects. Numerical results on 2D synthetic data are presented in the last section.

VISCOACOUSTIC WAVE EQUATION IN TTI MEDIA

In 2D case, the first order viscoacoustic wave equations of TTI media is expressed as follow (Fathalian and Innanen, 2017)

$$\partial_t u_x = \frac{1}{\rho}(\cos\theta\cos\varphi\partial_x - \sin\theta\partial_z)\sigma_H, \tag{1}$$

$$\partial_t u_z = \frac{1}{\rho}(\cos\varphi\sin\theta\partial_x + \cos\theta\partial_z)\sigma_V, \tag{2}$$

$$\partial_t \sigma_H = \rho V_P^2 \left[(1+2\varepsilon) \left[\left(\frac{\tau_\varepsilon}{\tau_\sigma} \right) \left[(\cos\theta \cos\varphi \partial_x - \sin\theta \partial_z) u_x \right] - r_H \right] + \sqrt{1+2\delta} \left[(\cos\varphi \sin\theta \partial_x + \cos\theta \partial_z) u_z \right] \right], \quad (3)$$

$$\partial_t \sigma_V = \rho V_P^2 \left[\sqrt{1+2\delta} \left[(\cos\theta \cos\varphi \partial_x - \sin\theta \partial_z) u_x \right] + \left(\frac{\tau_\varepsilon}{\tau_\sigma} \right) \left[(\cos\varphi \sin\theta \partial_x + \cos\theta \partial_z) u_z + \right] - r_V \right], \quad (4)$$

where $u_x(x,t)$ and $u_z(x,t)$ are the particle velocity components in the x- and z-directions respectively. σ_H and σ_V represent the horizontal and vertical stress components respectivel, $P(x,t)$ is pressure wavefield, $\rho(x)$ is density, r is a memory variable, ε and δ are Thomsen parameters, K represents the bulk modulus of the medium, and θ represent the tilt angle and φ represent the azimuth of tilt for TTI symmetry axithe. $r_{H\ell}$, and $r_{V\ell}$, which are referred to as memory variables of horizontal and vertical stress components (Carcione et al., 1988), satisfy

$$\partial_t r_{H\ell} = -\frac{1}{\tau_{\sigma\ell}} r_{H\ell} + \rho V_p^2 \left((\cos\theta \cos\varphi \partial_x - \sin\theta \partial_z) u_x \right) \frac{1}{\tau_{\sigma\ell}} \left(1 - \frac{\tau_{\varepsilon\ell}}{\tau_{\sigma\ell}} \right), \quad (5)$$

$$\partial_t r_{V\ell} = -\frac{1}{\tau_{\sigma\ell}} r_{V\ell} + \rho V_p^2 \left((\cos\varphi \sin\theta \partial_x + \cos\theta \partial_z) u_z \right) \frac{1}{\tau_{\sigma\ell}} \left(1 - \frac{\tau_{\varepsilon\ell}}{\tau_{\sigma\ell}} \right) .1 \leq \ell \leq L,$$

The stress and strain relaxation parameters, τ_ε and τ_σ, are related to the quality factor Q and the reference angular frequency ω as (Robertsson et al., 1994)

$$\tau_\sigma = \frac{\sqrt{1+1/Q^2} - 1/Q}{\omega}, \quad (6)$$
$$\tau_\varepsilon = \frac{1}{\omega^2 \tau_\sigma}.$$

where ω is the central frequency of the source wavelet.
In attenuation media, there are two main visible effects, reduced amplitude and phase shift due to dispersion. Therefore, the simulation of wave propagation includes three cases, i.e., the amplitude loss effect, the phase dispersion effect, or both effects. In this paper, we present a new approach for the solution of the viscoacoustic wave equation in the time domain to explicitly separate phase dispersion and amplitude attenuation. We first apply the Fourier transform to the first-order linear differential equations 1, 2, 3, 4, and 5 in the time domain to obtain the frequency domain viscoacoustic wave equation:

$$\tilde{u}_x = \frac{1}{\rho} (\cos\theta \cos\varphi \partial_x - \sin\theta \partial_z) \tilde{\sigma}_H, \quad (7)$$

$$\tilde{u}_z = \frac{1}{\rho} (\cos\varphi \sin\theta \partial_x + \cos\theta \partial_z) \tilde{\sigma}_V, \quad (8)$$

$$i\omega\tilde{\sigma}_H = \rho V_P^2 \left[(1+2\varepsilon) \left[\left(\frac{\tau_\varepsilon}{\tau_\sigma} \right) \left[(\cos\theta\cos\varphi\partial_x - \sin\theta\partial_z)\tilde{u}_x \right] - \tilde{r}_H \right] + \sqrt{1+2\delta} \left[(\cos\varphi\sin\theta\partial_x + \cos\theta\partial_z)\tilde{u}_z \right] \right], \quad (9)$$

$$i\omega\tilde{\sigma}_V = \rho V_P^2 \left[\sqrt{1+2\delta} \left[(\cos\theta\cos\varphi\partial_x - \sin\theta\partial_z)\tilde{u}_x \right] + \left(\frac{\tau_\varepsilon}{\tau_\sigma} \right) \left[(\cos\varphi\sin\theta\partial_x + \cos\theta\partial_z)\tilde{u}_z \right] - \tilde{r}_V \right], \quad (10)$$

$$i\omega\tilde{r}_{H\ell} = -\frac{1}{\tau_{\sigma\ell}}\tilde{r}_{H\ell} + \rho V_p^2 \left((\cos\theta\cos\varphi\partial_x - \sin\theta\partial_z)\tilde{u}_x \right) \frac{1}{\tau_{\sigma\ell}} \left(1 - \frac{\tau_{\varepsilon\ell}}{\tau_{\sigma\ell}} \right), \quad (11)$$

$$i\omega\tilde{r}_{V\ell} = -\frac{1}{\tau_{\sigma\ell}}\tilde{r}_{V\ell} + \rho V_p^2 \left((\cos\varphi\sin\theta\partial_x + \cos\theta\partial_z)\tilde{u}_z \right) \frac{1}{\tau_{\sigma\ell}} \left(1 - \frac{\tau_{\varepsilon\ell}}{\tau_{\sigma\ell}} \right) .1 \leq \ell \leq L, \quad (12)$$

From equations 11 and 12, the memory variable in the frequency domain can be calculated as a function of the particle velocity and the relaxation time

$$\tilde{r}_{H\ell} = \rho V_p^2 \left((\cos\theta\cos\varphi\partial_x - \sin\theta\partial_z)\tilde{u}_x \right) \frac{\tau_\sigma^{-1}\left(1 - \tau_\varepsilon\tau_\sigma^{-1}\right)}{(i\omega + \tau_\sigma^{-1})}, \quad (13)$$

$$\tilde{r}_{V\ell} = \rho V_p^2 \left((\cos\varphi\sin\theta\partial_x + \cos\theta\partial_z)\tilde{u}_z \right) \frac{\tau_\sigma^{-1}\left(1 - \tau_\varepsilon\tau_\sigma^{-1}\right)}{(i\omega + \tau_\sigma^{-1})}). \quad (14)$$

By substituting the equations 13 and 14 into equations 9 and 10 respectively, the memory variable equations are removed. Therefore, a set of first-order differential equations includes now only four equations, resulting in less computational time. The new first-order viscoacoustic wave equation in the frequency domain is

$$i\omega\tilde{\sigma}_H = \rho V_P^2 \left[(1+2\varepsilon) \left[\left(\frac{\tau_\varepsilon}{\tau_\sigma} - \frac{\frac{1}{\tau_\sigma}\left(\frac{\tau_\varepsilon}{\tau_\sigma} - 1\right)}{i\omega + \frac{1}{\tau_\sigma}} \right) \left[(\cos\theta\cos\varphi\partial_x - \sin\theta\partial_z)\tilde{u}_x \right] \right] + \sqrt{1+2\delta} \left[(\cos\varphi\sin\theta\partial_x + \cos\theta\partial_z)\tilde{u}_z \right] \right], \quad (15)$$

$$i\omega\tilde{\sigma}_V = \rho V_P^2 \left[\sqrt{1+2\delta} \left[(\cos\theta\cos\varphi\partial_x - \sin\theta\partial_z)\tilde{u}_x \right] + \left(\frac{\tau_\varepsilon}{\tau_\sigma} - \frac{\frac{1}{\tau_\sigma}\left(\frac{\tau_\varepsilon}{\tau_\sigma} - 1\right)}{i\omega + \frac{1}{\tau_\sigma}} \right) \left[(\cos\varphi\sin\theta\partial_x + \cos\theta\partial_z)\tilde{u}_z \right] \right], \quad (16)$$

After some algebra manipulation, the viscoacoustic TTI wave equations in the frequency domain are simplified as

$$i\omega\tilde{\sigma}_H = \rho V_P^2 \left[(1+2\varepsilon)\left[\left(\frac{(\omega^2\tau_\varepsilon\tau_\sigma+1)}{\omega^2\tau_\sigma^2+1}+i\frac{(\omega\tau_\epsilon-\omega\tau_\sigma)}{\omega^2\tau_\sigma^2+1}\right)[(\cos\theta\cos\varphi\partial_x-\sin\theta\partial_z)\tilde{u}_x]\right]\right.$$
$$\left.+\sqrt{1+2\delta}\,[(\cos\varphi\sin\theta\partial_x+\cos\theta\partial_z)\tilde{u}_z]\right], \quad (17)$$

$$i\omega\tilde{\sigma}_V = \rho V_P^2 \left[\sqrt{1+2\delta}\,[(\cos\theta\cos\varphi\partial_x-\sin\theta\partial_z)\tilde{u}_x]\right.$$
$$\left.+\left(\frac{(\omega^2\tau_\varepsilon\tau_\sigma+1)}{\omega^2\tau_\sigma^2+1}+i\frac{(\omega\tau_\epsilon-\omega\tau_\sigma)}{\omega^2\tau_\sigma^2+1}\right)[(\cos\varphi\sin\theta\partial_x+\cos\theta\partial_z)\tilde{u}_z]\right], \quad (18)$$

Equations 17 and 18 are transformed back to the time domain to derive the viscoacoustic TTI wave equation that maintains the approximate constant-Q attenuation and dispersion behaviours during wave propagation. To apply these equations on RTM, we write the viscoacoustic wave equation in TTI media for the forward and backward extrapolation as:

$$\partial_t\sigma_H = \rho V_P^2 \left[(1+2\varepsilon)\left[(a_1(2/A)+ia_2(2/AQ))\left[(\cos\theta\cos\varphi\partial_x-\sin\theta\partial_z)u_x\right]\right]\right.$$
$$\left.+\sqrt{1+2\delta}\,[(\cos\varphi\sin\theta\partial_x+\cos\theta\partial_z)u_z]\right], \quad (19)$$

$$\partial_t\sigma_V = \rho V_P^2 \left[\sqrt{1+2\delta}\,[(\cos\theta\cos\varphi\partial_x-\sin\theta\partial_z)u_x]\right.$$
$$\left.+(a_1(2/A)+ia_2(2/AQ))\left[(\cos\varphi\sin\theta\partial_x+\cos\theta\partial_z)u_z\right]\right], \quad (20)$$

where $A=\sqrt{1+1/Q^2}-1/Q)^2+1$. $2/A$ and $2/AQ$ are dispersion-dominated and amplitude-attenuation-dominated operators, respectively. The coefficients a_1 and a_2 are constants equal to 1. The sign of these coefficients is important for the forward and backward extrapolation. Note that when $Q \ll$, the dispersion-dominated operator goes to 1 and the amplitude-loss-dominated operator disappears, i.e., the viscoacoustic case approaches to the acoustic case. To show the decoupled velocity dispersion and amplitude loss, we consider a homogeneous model with a background velocity of 2500 m/s and quality factor Q=10. The source is located in the center of the model, and the source signature is a zero-phase Ricker wavelet with a central frequency of 25 Hz. The grid spacing in the x and z directions is 4 m, and the Thomsen anisotropic parameters $\varepsilon = 0.2$ and $\delta = 0.05$. Figure 1 corresponds to an axis of symmetry tilting at 45. The compressional P wavefront is approximately ellipsoidal, and the shear wave artifacts generated in an elliptic media is suppressed at the source by design a small smoothly tapered circular region with $\varepsilon = \delta$ around the source. However, to avoid the numerical computation instability in TTI media, we applying the viscoacoustic equation and simply setting the shear wave velocity along the tilted symmetry axis to zero (pure P wave equation). The snapshot of the acoustic reference wavefield is shown in Figure 1a. The dashed yellow line indicates the wavefront. The

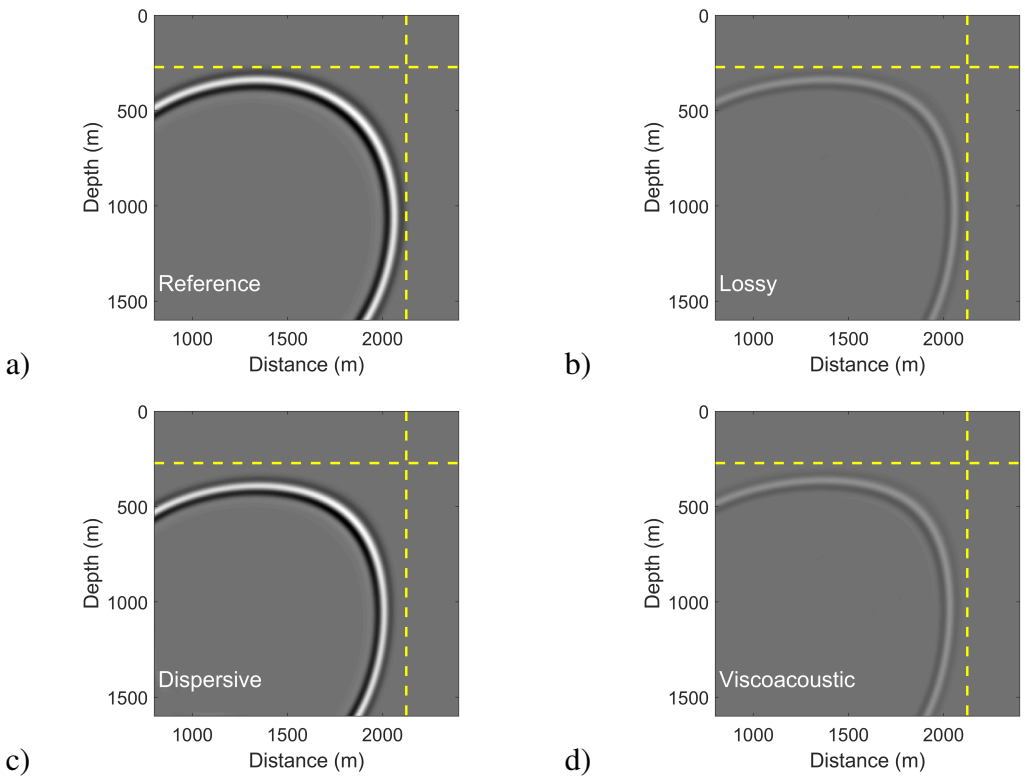

FIG. 1: 2D wavefield snapshots using (a) acoustic, (b) amplitude loss, (c) dispersive, and (d) viscoacoustic in a TTI medium with $\varepsilon = 0.2$, $\delta = 0.05$, and $\theta = 45$.

amplitude-loss simulation (imaginary part of equations 19 and 20) is shown in figure 1b. Compared with the acoustic case, the amplitude is attenuated, but the phases are the same. In figure 1c the phase dispersion simulation (real part of equations 19 and 20) is shown. The phase has a shift, and the amplitude is similar to the acoustic case. In figure 1d the viscoacoustic wavefield using equation 1-5 is displayed. The reduced amplitude and shifted phase are visible compared with the acoustic reference wavefield. Thus, using the viscoacoustic wave equation in TTI media with decoupling attenuation and dispersion terms, we can compensate the amplitude loss and dispersion in images separately, which is explained in the RTM section.

VISCOACOUSTIC REVERSE TIME PROPAGATION

Reverse-time migration reconstructs the receiver wavefield by backwards propagating the measured seismic data at the receiver. The amplitude of the back propagation waves in attenuation media is reduced, and it needs to be amplified. The positive sign of the a_2 constant refers to the amplitude attenuation in extrapolating forward propagation. By reversing the sign of the amplitude attenuation term ($a_2 = -1$) in the viscoacoustic TTI wave equation, we can compensate for the amplitude loss. Also, the viscoacoustic wave equation contains the dispersion term that affects the phase during wave propagation, but the sign of this term ($a_1 = 1$) is not changed.
For the backward modelling, the viscoacoustic TTI wave equations with compensation of

attenuation effects ($a_1 = 1$ and $a_2 = -1$) can be written as

$$\partial_t \sigma_H = \rho V_P^2 \left[(1+2\varepsilon) \left[(a_1(2/A) - i a_2(2/AQ)) \left[(\cos\theta \cos\varphi \partial_x - \sin\theta \partial_z) u_x \right] \right] \right.$$
$$\left. + \sqrt{1+2\delta} \left[(\cos\varphi \sin\theta \partial_x + \cos\theta \partial_z) u_z \right] \right], \quad (21)$$

$$\partial_t \sigma_V = \rho V_P^2 \left[\sqrt{1+2\delta} \left[(\cos\theta \cos\varphi \partial_x - \sin\theta \partial_z) u_x \right] \right.$$
$$\left. + (a_1(2/A) - i a_2(2/AQ)) \left[(\cos\varphi \sin\theta \partial_x + \cos\theta \partial_z) u_z \right] \right], \quad (22)$$

Using the phase dispersion part, the phase only viscoacoustic TTI wave equation will be

$$\partial_t \sigma_H = \rho V_P^2 \left[(1+2\varepsilon) \left[(a_1(2/A)) \left[(\cos\theta \cos\varphi \partial_x - \sin\theta \partial_z) u_x \right] \right] \right.$$
$$\left. + \sqrt{1+2\delta} \left[(\cos\varphi \sin\theta \partial_x + \cos\theta \partial_z) u_z \right] \right], \quad (23)$$

$$\partial_t \sigma_V = \rho V_P^2 \left[\sqrt{1+2\delta} \left[(\cos\theta \cos\varphi \partial_x - \sin\theta \partial_z) u_x \right] \right.$$
$$\left. + (a_1(2/A)) \left[(\cos\varphi \sin\theta \partial_x + \cos\theta \partial_z) u_z \right] \right], \quad (24)$$

To compensate for the amplitude attenuation effect only, we keep the imaginary part of equation 19 and 20, so that the viscoacoustic TTI wave equation for back-propagation will be

$$\partial_t \sigma_H = \rho V_P^2 \left[(1+2\varepsilon) \left[(-a_2(2/AQ)) \left[(\cos\theta \cos\varphi \partial_x - \sin\theta \partial_z) u_x \right] \right] \right.$$
$$\left. + \sqrt{1+2\delta} \left[(\cos\varphi \sin\theta \partial_x + \cos\theta \partial_z) u_z \right] \right], \quad (25)$$

$$\partial_t \sigma_V = \rho V_P^2 \left[\sqrt{1+2\delta} \left[(\cos\theta \cos\varphi \partial_x - \sin\theta \partial_z) u_x \right] \right.$$
$$\left. + (-a_2(2/AQ)) \left[(\cos\varphi \sin\theta \partial_x + \cos\theta \partial_z) u_z \right] \right], \quad (26)$$

Combining equations 1, 2, 19 and 20 (with t replaced by $-t$), we obtain the viscoacoustic backward modeling equation, i.e., the solution of $u_{x,z}(\mathbf{X}, -t)$, $\mathbf{X}$ refer to x and z for 2D, is the time-reversed version of the solution $u_{x,z}(\mathbf{X}, t)$ of the forward propagation equations 8, 9, and 20. For the backward modeling, we solve equation 21 to extrapolate the receiver wavefield by flipping in time the measured data $R(\mathbf{X}_r, t)$ at the receivers with a boundary condition.

2D SYNTHETIC EXAMPLES

We examine the new approach of Q-RTM using a layered model and then apply this approach to the complex Marmousi model using a time-space domain FD method. Figures 2a and 2b show the true and migration velocity models with a Q anomaly for the

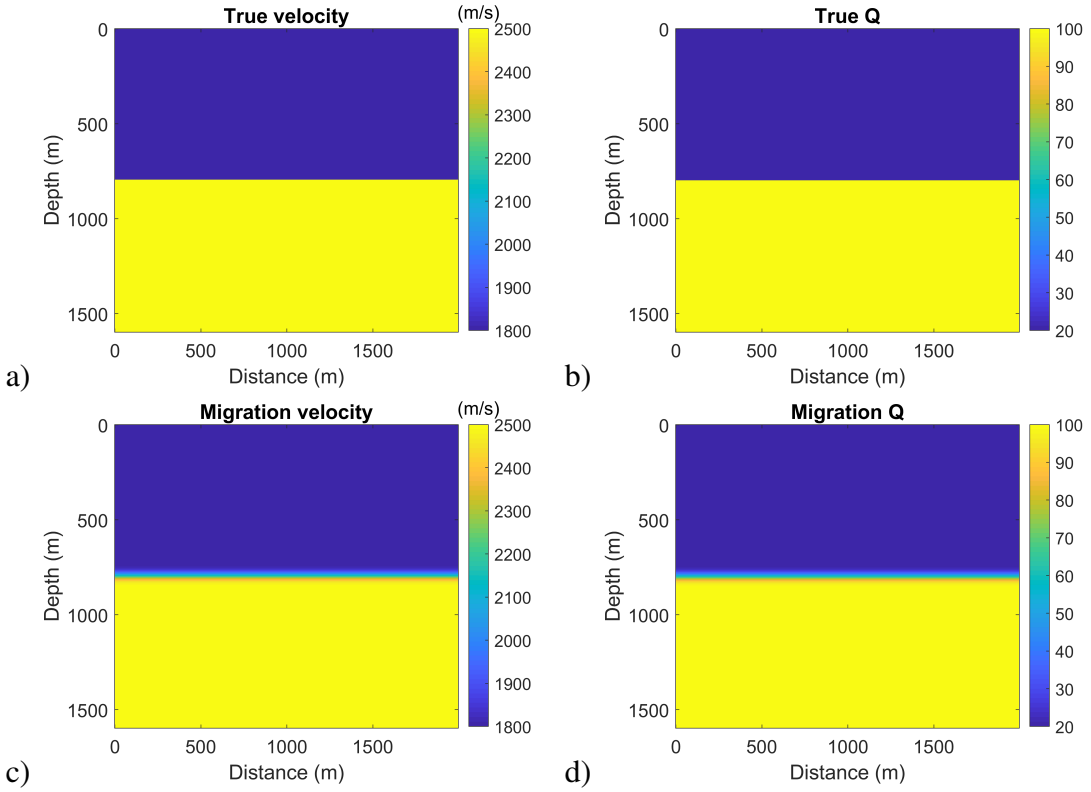

FIG. 2: (a) True velocity model, (b) True Q model, (c) migration velocity model, and (d) migration Q model.

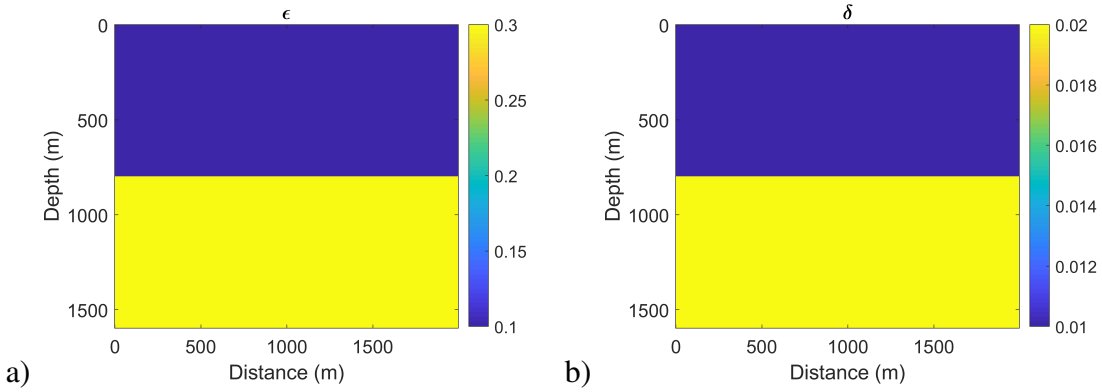

FIG. 3: Transversely isotropic layered velocity model. a) Thomsen's ε model, b) Thomsen's δ model.

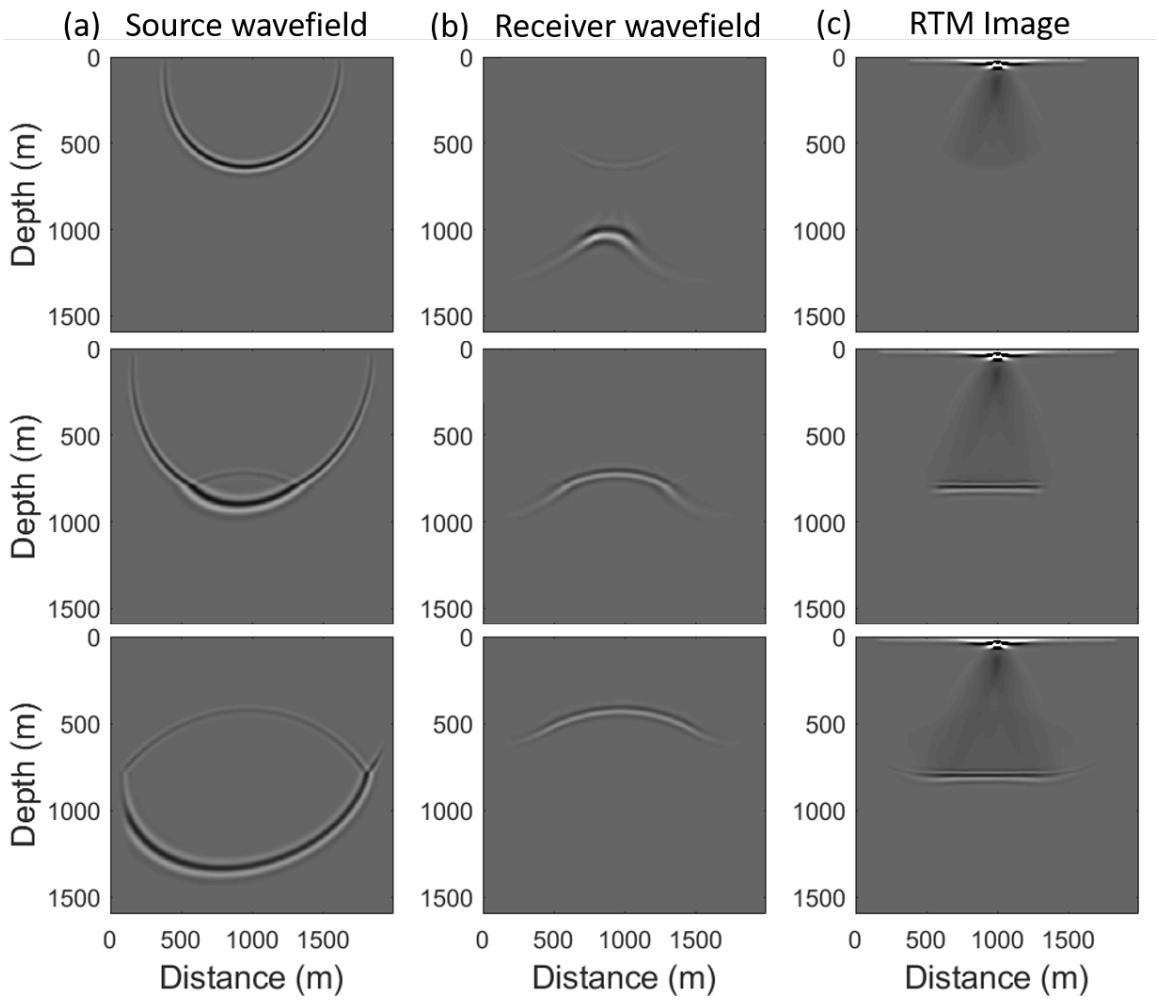

FIG. 4: Reference snapshots of the source wavefield, the receiver wavefield, and the RTM image at 0.5, 0.62, and 0.79 s. The acoustic data in TTI media are extrapolated for the receiver wavefield using the acoustic RTM.

layered model. The model grid dimensions are 401×501, the grid size is 4 m$\times$4 m, and the Thomsen anisotropic parameters are shown ion figures 3. The sampling interval is 0.8 ms, and the recording length is 1.5 s. As the source we use a zero-phase Ricker wavelet with a center frequency of 25 Hz. Perfectly matched layer (PML) absorbing boundary conditions are used to attenuate the reflections from an artificial boundary. The front wave of the P wave presents an elliptical shape because of the anisotropic effect. There is a problem due to shear wave that generated by the source, which for the acoustic and viscoacoustic medium have to regarded as artifacts(Alkhalifah, 2000; Grechka et al., 2004).

The shear wave artifacts generated in an elliptic media ($\varepsilon \neq \delta$), and they can suppress at the source by design a small smoothly tapered circular region with $\varepsilon = \delta$ around the source. To show the application of Q-RTM approach, we present the snapshots of the source wavefield, the receiver wavefield, and RTM images in attenuation media and compare with the reference one. Figure 4 shows the reference snapshot results using acoustic RTM at different time step. To obtain the RTM image the acoustic data are extrapolated for the receiver

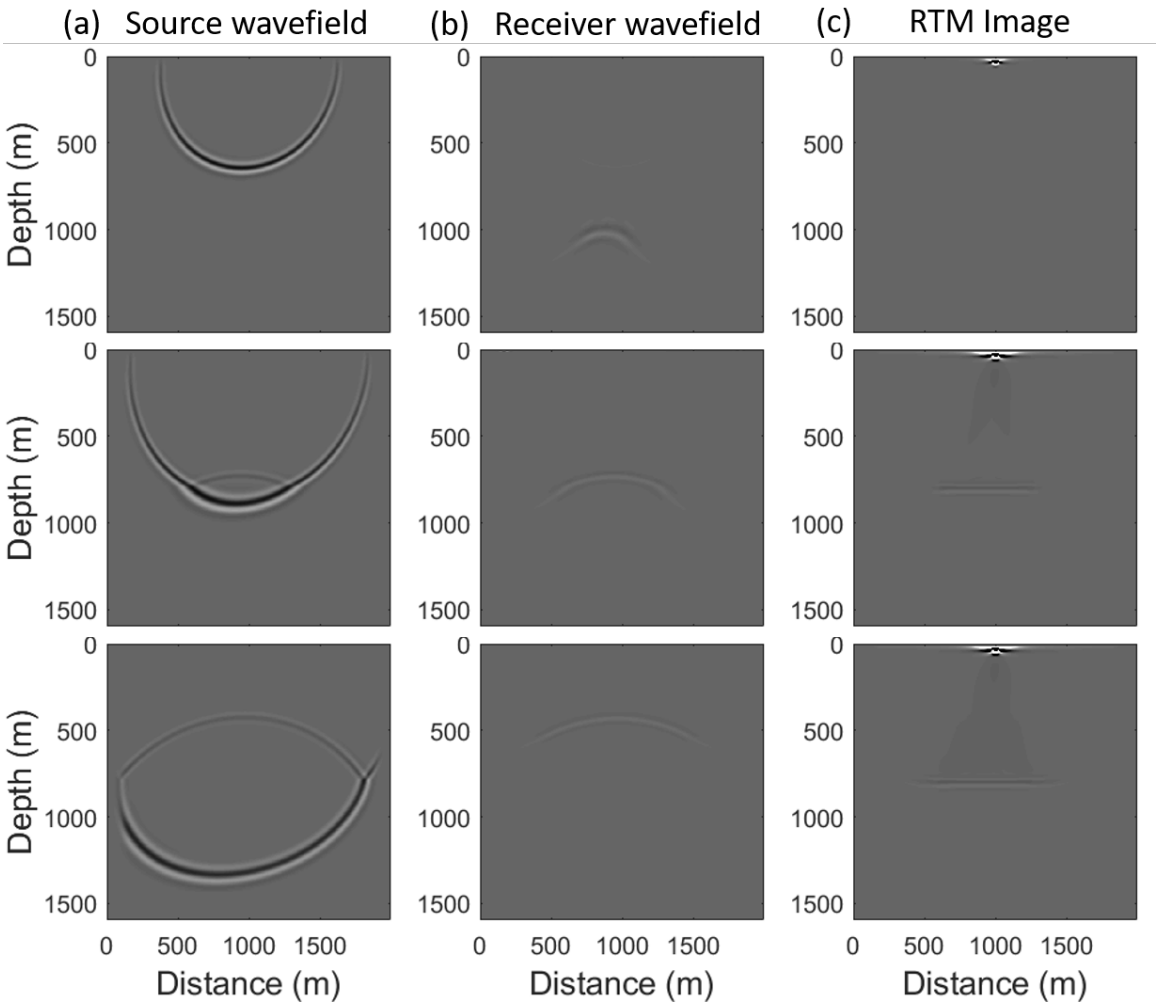

FIG. 5: Snapshots of the source wavefield, the receiver wavefield, and the RTM image at 0.5, 0.62, and 0.79 s. The viscoacoustic data are extrapolated for the receiver wavefield using acoustic RTM.

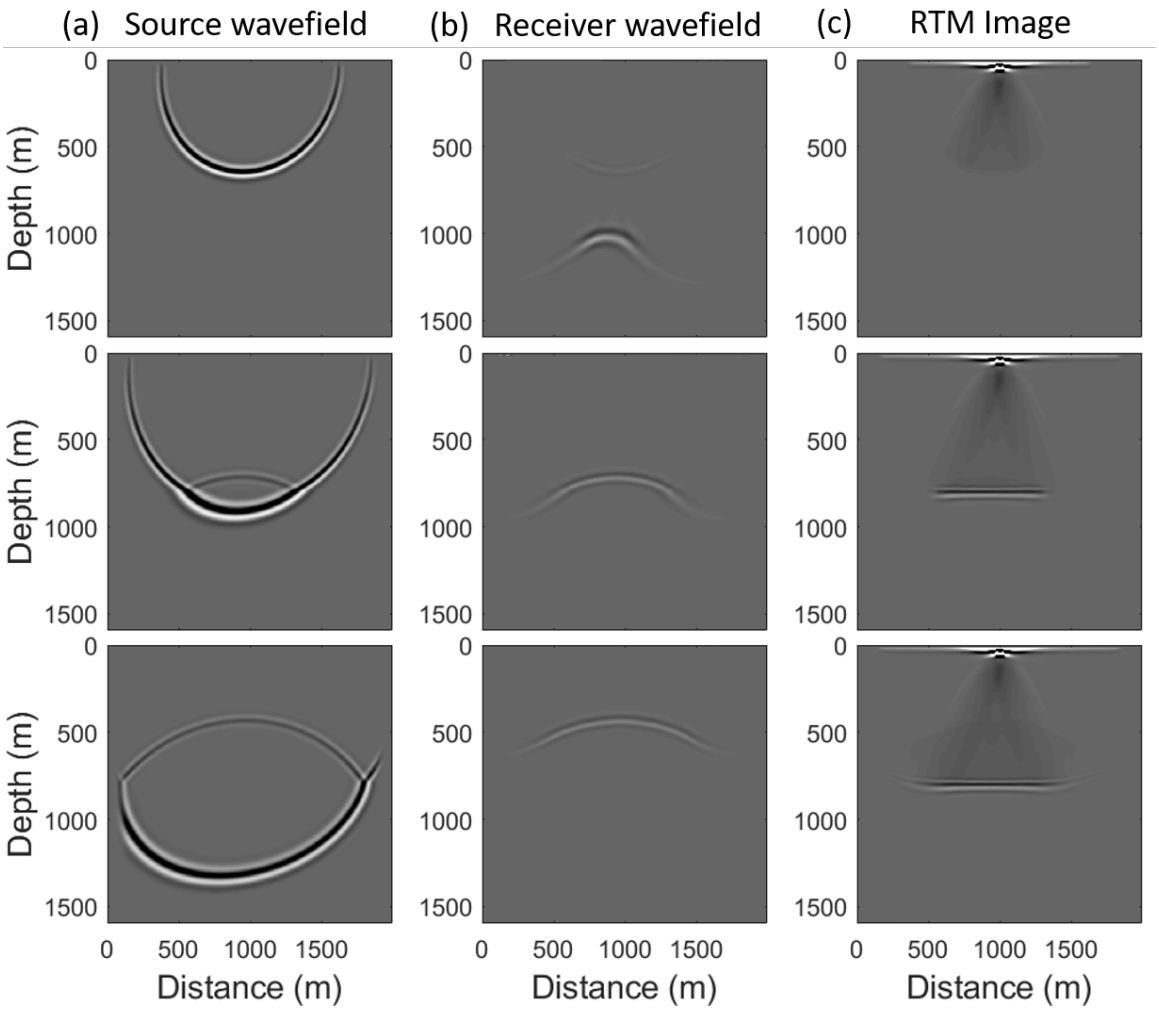

FIG. 6: Snapshots of the source wavefield, the receiver wavefield, and the RTM image at 0.5, 0.62, and 0.79 s. The viscoacoustic data are extrapolated for the receiver wavefield using Q-RTM to compensate for the amplitude during extrapolating.

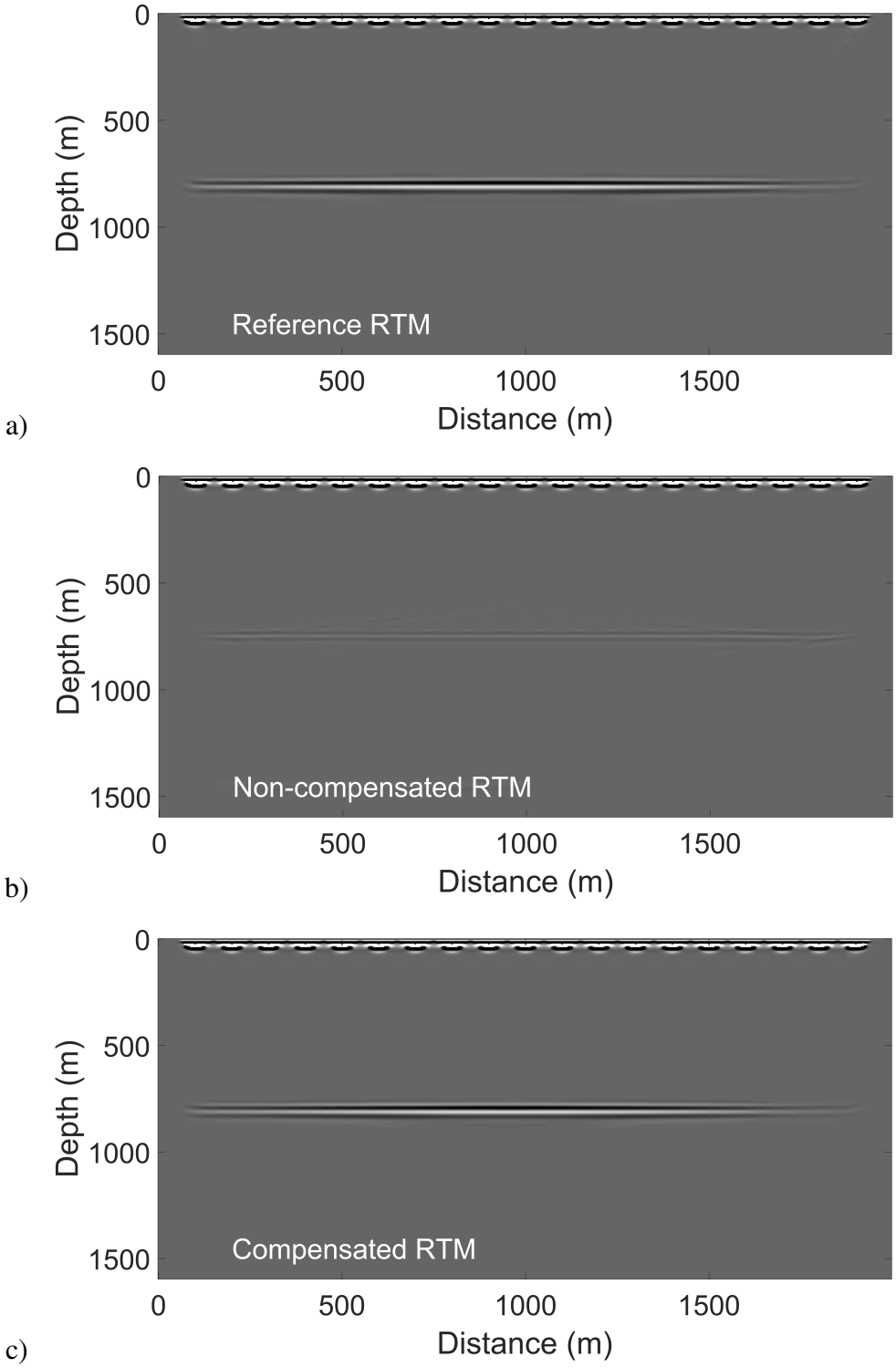

FIG. 7: Comparison among from (a) acoustic RTM (reference), (b) acoustic RTM with viscoacoustic data, and (c) Q-RTM with viscoacoustic data. The compensated case agree with the reference image very well.

wavefields. The anisotropy affects the wavefront of the P wave. Figure 5 shows the acoustic RTM using the viscoacoustic data. There are two main attenuation effects, reduced amplitude and shifted phase due to velocity dispersion. The receiver wavefield shows reduced wave amplitude while the source wavefield is comparable to the reference result. Hence, the RTM images at different time step show poor illumination. To improve image resolution, we test the new approach of Q-RTM on viscoacoustic data. Figure 6 shows the snapshots of source wavefield, receiver wavefield, and RTM image. Results show the amplitude of the source wavefield and receiver wavefield are amplified while the receiver wavefield is still weaker than the reference result because of incomplete compensation. However, the Q-RTM images are compensated and comparable to the reference images. To demonstrate the effect of attenuation, we apply viscoacoustic RTM to the viscoacoustic data set to generate the RTM image shown in Figure 7 and compare with the acoustic RTM image as the reference. The velocity and Q models are first smoothed from true models and then used for migration. In acoustic RTM with viscoacoustic data (noncompensated RTM) (Figure 7b), there is one reflector in the RTM-image with amplitude loss. The high-attenuation anomaly causes a reduction in wave amplitude, so migrating the attenuated data produces the weak reflectors. To solve the poor illumination problem of viscoacoustic RTM images, we apply for attenuation compensation during wave propagation using the new Q-RTM approach (equations 19 and 20). The compensated image using Q-RTM approach is shown in Figure 7c. The result indicates improved RTM image with recovered amplitudes of the reflectors at the dip depths compared with the reference image in Figure 7a. After compensation, the events have corrected amplitudes and corrected phases.

In the second example, we consider the more complex Marmousi model to verify the accuracy of the Q-RTM approach in TTI media. Figure 8 shows the actual and migration velocity models and the corresponding true and migration Q models. In the Q model, there are some regions that attenuate waves travelling through them and creating reflections with weaker amplitudes for the deeper layers, especially beneath strongly attenuating layers. Two anisotropy distributions are shown in Figure 9. By setting the tilt angle to be 45 degrees, the synthetic viscoacoustic TTI dataset is produced using equations 19 and 20. To avoid shear wave artifacts, we set a small smoothly tapered circular region with $\varepsilon = \delta$ around the source (Duveneck et al., 2008). The model grid dimensions are 281×701, and the grid size is 10 m$\times$10 m. Perfectly matched layer (PML) absorbing boundary conditions are used to attenuate the reflections from the model boundaries. We set 50 sources positioned at a depth of 30 m and a zero-phase Ricker wavelet with a centre frequency of 15 Hz. The sampling interval rate is 0.4 ms, and the recording length is 3 s. To remove the effect of S-wave that generated at the source the source is located in the isotropic part of the model, i.e., $\varepsilon = \delta$. The RTM images represented in Figure 10, which includes the acoustic RTM without attenuation (reference case), the acoustic RTM with viscoacoustic data (noncompensated case), and the compensated RTM using Q-RTM approach. The reference RTM image (Figure 10a) has similar artifacts and amplitudes in the shallow layers compared with the noncompensated RTM image, but the non-compensated case in Figure 10b has very weak amplitudes in the deeper layers especially beneath the layers with strong attenuation. The attenuation affects the amplitudes and the phases of the propagating waves, effects which are not taken into account in the acoustic RTM image. The Q-compensated RTM image is shown in Figure 10c. The result indicates improved RTM image with re-

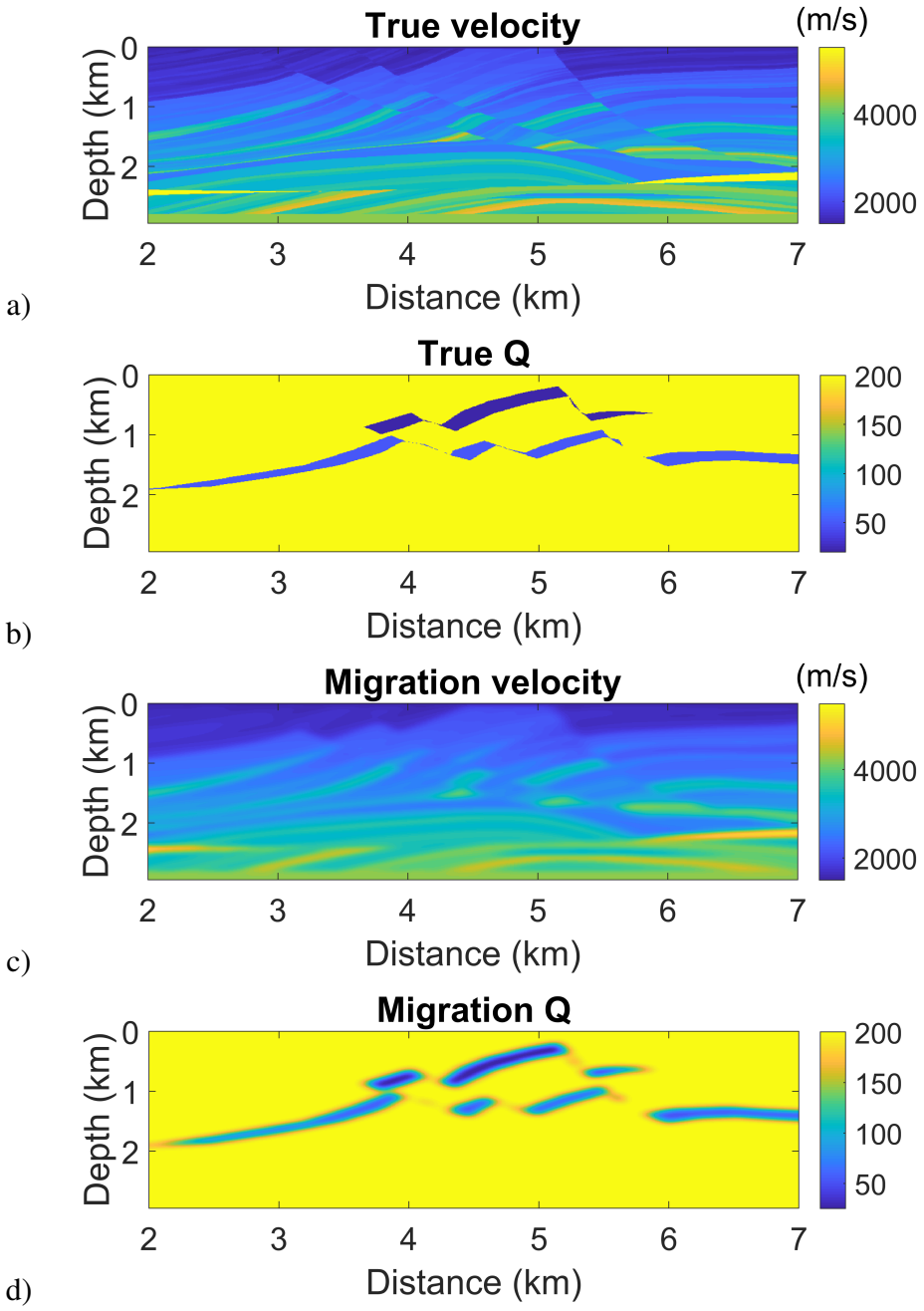

FIG. 8: The Marmousi models: (a) true velocity model, (b) true Q model, (c) migration velocity model, and (d) migration model.

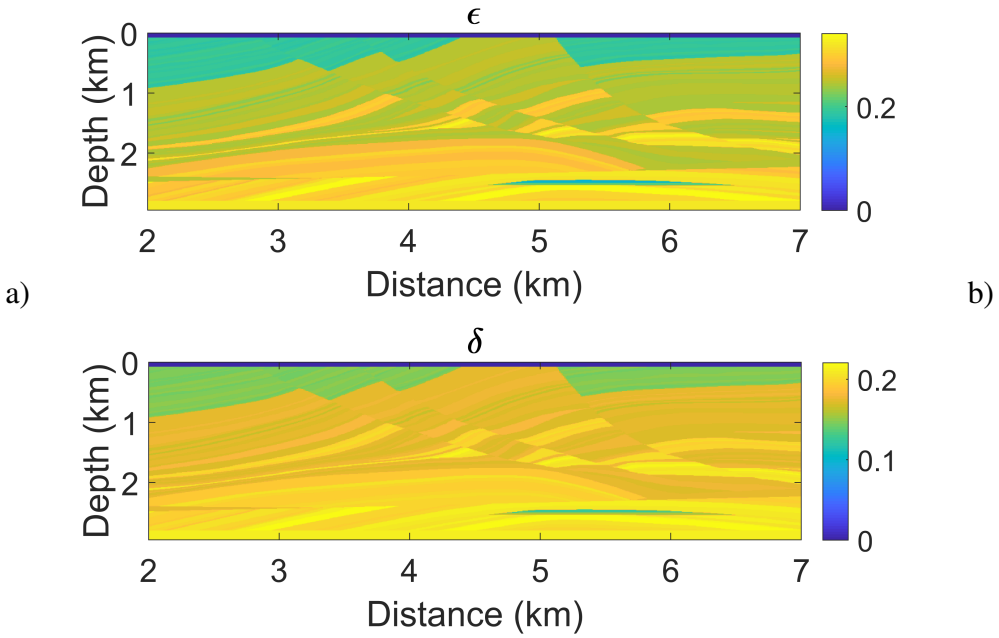

FIG. 9: Transversely isotropic Marmousi velocity model. a) Thomsen's ε model, b) Thomsen's δ model

covered amplitudes of the reflectors at the dip depths compared with the reference image in Figure 10a. To verify that the reflectors migrated to the correct position we compare the image traces at the same offset. Right panels of Figure 10 show comparisons traces from the RTM images at offset 4.2 km. The non-compensated trace (solid red line) have a shifted phase and reduced amplitude. The compensated traces (solid green line) is more correct in amplitude and phase compared to the reference one (solid blue line). Both of these examples show that the proposed Q-RTM approach in TTI media is useful to compensate the amplitude loss and shifted phase due to attenuation effects.

CONCLUSIONS

We have presented a viscoacoustic RTM imaging algorithm in tilted TI media based on the time-domain constant-Q wave propagation involving a series of standard linear solid mechanisms that can mitigate the attenuation and dispersion effects in the migrated images. The wave equations have been extended from isotropic media to tilted TI media. The amplitude loss and phase dispersion in the source and receivers wavefields can be recovered by applying compensation operators on the measured receiver wavefield. The phase dispersion and amplitude attenuation operators in Q-RTM approach are separated, and the compensation operators are constructed by reversing the sign of the attenuation operator without changing the sign of the dispersion operator. It is clear that TTI Q-RTM can produce a more accurate image than isotropic RTM, especially in areas with anisotropy, attenuation and strong variations of dip angle. Numerical tests on synthetic data illustrate that this Q-RTM approach in TTI media can improve the image resolution, particularly beneath areas with strong attenuation.

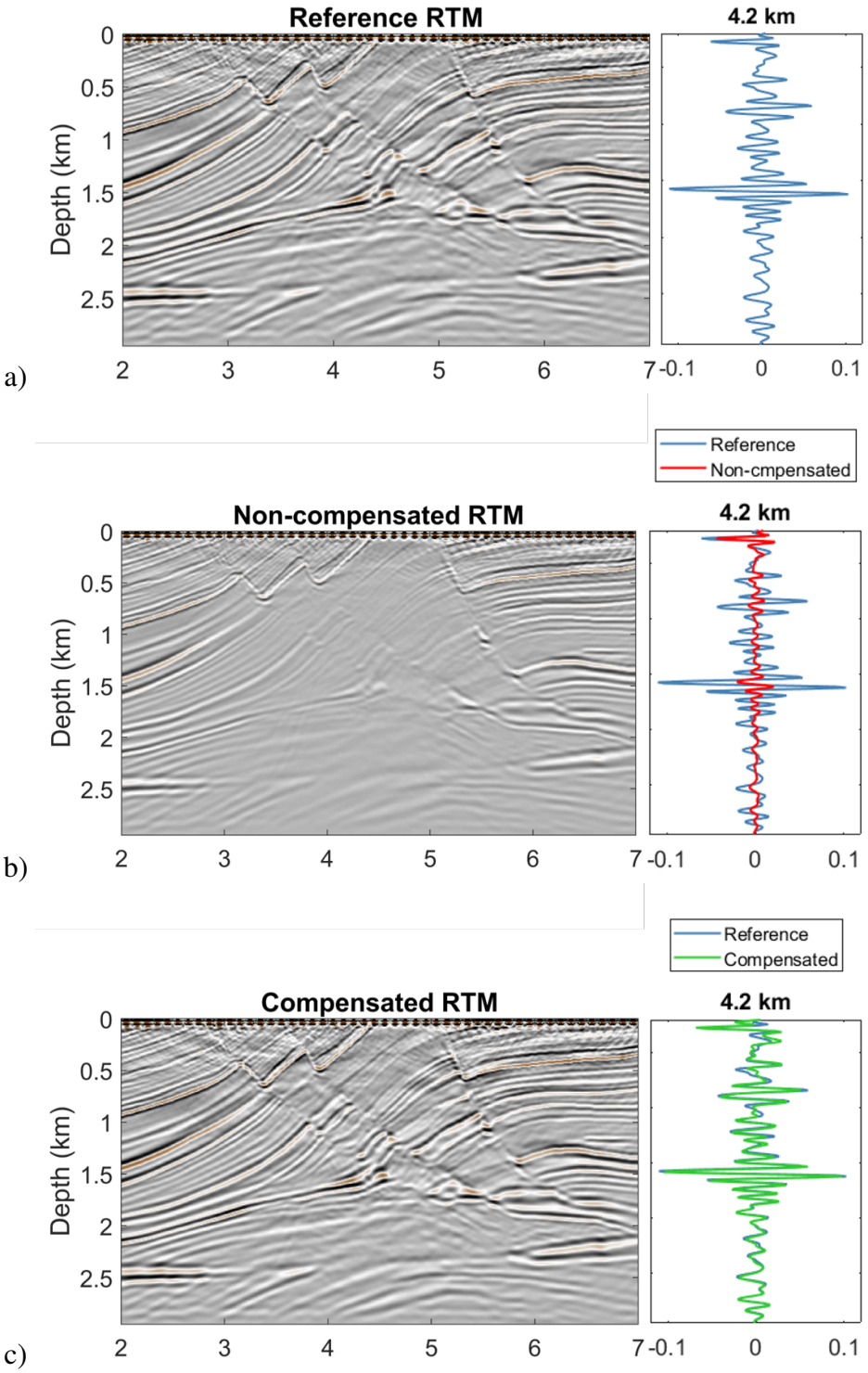

FIG. 10: Comparison among from (a) acoustic RTM (reference), (b) acoustic RTM with viscoacoustic data, and (c) Q-RTM with viscoacoustic data. The right panels show the reference trace (blue line), non-compensated trace (red line), and compensated trace (green line)at the horizontal 4.2 km. The compensated case agree with the reference image very well.

ACKNOWLEDGMENTS

The authors thank the sponsors of CREWES for continued support. This work was funded by Mitacs, CREWES industrial sponsors and NSERC (Natural Science and Engineering Research Council of Canada) through the grant CRDPJ 461179-13.

REFERENCES

Alkhalifah, T., 1998, Acoustic approximations for processing in transversely isotropic media: Geophysics, **63**, 623–631.

Alkhalifah, T., 2000, An acoustic wave equation for anisotropic media: Geophysics, **67**, 1304–1325.

Blanch, J. O., and Symes, W. W., 1995, Efficient iterative viscoacoustic linearized inversion, *in* SEG Technical Program Expanded Abstracts 1995, Society of Exploration Geophysicists, 627–630.

Carcione, J. M., Kosloff, D., and Kosloff, R., 1988, Viscoacoustic wave propagation simulation in the earth: Geophysics, **53**, 769–777.

Crampin, S., 1984, Anisotropy in exploration seismics, journal = First Break, volume = 2, pages = 19–21.

Dutta, G., and Schuster, G. T., 2014, Attenuation compensation for least-squares reverse time migration using the viscoacoustic-wave equation: Geophysics, **79**, No. 6, S251–S262.

Duveneck, E., Milcik, P., Bakker, P. M., and Perkins, C., 2008, Acoustic vti wave equa- tions and their application for anisotropic reverse-time migration: SEG Technical Program Expanded Abstracts, **27**, 2186–2190.

Fathalian, A., and Innanen, K., 2017, Viscoacoustic vti and tti wave equations and their application for anisotropic reverse time migration: Constant-q approximation: CREWES reports, **29**.

Fletcher, R., Du, X., and Fowler, P. J., 2008, A new pseudo-acoustic wave equation for ti media: SEG Technical Program Expanded Abstracts, **27**, 2082–2086.

Fletcher, R., Du, X., and Fowler, P. J., 2009, Reverse time migration in tilted transversely isotropic (tti) media: Geophysics, **74**, WCA179–WCA187.

Fletcher, R., Nichols, D., and Cavalca, M., 2012, Wavepath-consistent effective q estimation for q-compensated reverse-time migration, *in* 74th EAGE Conference and Exhibition incorporating EUROPEC 2012.

Grechka, V., Zhang, L., and Rector, J. W., 2004, Shear waves in acoustic anisotropic media: Geophysics, **69**, 576–582.

Robertsson, J. O. A., Blanch, J. O., and Symes, W. W., 1994, Viscoelastic finite-difference modeling: Geophysics: Geophysics, **59**, 1444–1456.

Yoon, K., Suh, S., Ji, J., Cai, J., and Wang, B., 2010, Stability and speedup issues in tti rtm implementation: SEG Technical Program Expanded Abstracts, **29**, 3221–3225.

Zhang, H., and Zhang, Y., 2008, Reverse time migration in 3d heterogeneous tti media: SEG Technical Program Expanded Abstracts,, **27**, 2196–2200.

Zhou, H., Zhang, G., and Bloor, R., 2006.

Zhu, T., and Harris, J. M., 2014, Modeling acoustic wave propagation in heterogeneous attenuating media using decoupled fractional laplacians: Geophysics, **79**, No. 3, T105–T116.